Silver doping of silica-hafnia waveguides containing Tb^{3+}/Yb^{3+} rare earths for downconversion in PV solar cells

F. Enrichi [a, b, c, d, *], C. Armellini [c], G. Battaglin [b], F. Belluomo [e], S. Belmokhtar [f], A. Bouajaj [f], E. Cattaruzza [b], M. Ferrari [c, a], F. Gonella [a, b], A. Lukowiak [g], M. Mardegan [b], S. Polizzi [b], E. Pontoglio [b], G.C. Righini [a, h], C. Sada [i], E. Trave [b], L. Zur [a, c]

[a] *Museo Storico della Fisica e Centro Studi e Ricerche Enrico Fermi, Piazza del Viminale 1, 00184 Roma, Italy*
[b] *Dipartimento di Scienze Molecolari e Nanosistemi, Università Ca' Foscari Venezia, via Torino 155/b, 30172 Mestre, Venezia, Italy*
[c] *CNR-IFN, Istituto di Fotonica e Nanotecnologie, CSMFO Lab. & FBK-CMM, Via alla Cascata 56/C, 38123 Povo, Trento, Italy*
[d] *Division of Materials Science, Department of Engineering Sciences and Mathematics, Luleå University of Technology, 971 87 Luleå, Sweden*
[e] *Meridionale Impianti SpA, Via Senatore Simonetta 26/D, 20867 Caponago, Monza Brianza, Italy*
[f] *Laboratoire des Technologies Innovantes, LTI, Département de Génie industriel ENSA – Tanger, Université Abdelmalek Essaâdi, Tanger, Morocco*
[g] *Institute of Low Temperature and Structure Research, PAS, ul. Okolna 2, 50-422, Wroclaw, Poland*
[h] *IFAC-CNR Istituto di Fisica Applicata, Via Madonna del Piano 10, 50019, Sesto Fiorentino, FI, Italy*
[i] *Dipartimento di Fisica e Astronomia G. Galilei, Università di Padova, Via Marzolo 8, 35131, Padova, Italy*

ARTICLE INFO

Article history:
Received 7 July 2016
Accepted 29 July 2016

Keywords:
Downconversion
Optical waveguides
Photoluminescence
Ag doping
Tb–Yb rare earths
Solar cells

ABSTRACT

The aim of this paper is to study the possibility to obtain an efficient downconverting waveguide which combines the quantum cutting properties of Tb^{3+}/Yb^{3+} codoped materials with the optical sensitizing effects provided by silver doping. The preparation of $70SiO_2–30HfO_2$ glass and glass-ceramic waveguides by sol-gel route, followed by Ag doping by immersion in molten salt bath is reported. The films were subsequently annealed in air to induce the migration and/or aggregation of the metal ions. Results of compositional and optical characterization are given, providing evidence for the successful introduction of Ag in the films, while the photoluminescence emission is strongly dependent on the annealing conditions. These films could find potential applications as downshifting layers to increase the efficiency of PV solar cells.

1. Introduction

Solar energy has the great advantage of being inextinguishable, widely available across the planet and relatively cheap. Moreover, solar energy exploitation produces little or no wastes such as carbon dioxide or other chemical pollutants, thus having minimal environmental impact. For these reasons, strong efforts and research investments are devoted to improve their efficiency. Among solar exploitation systems, photovoltaic devices (PV) rely on the capability of the active material to absorb light and generate charge carriers, and on the subsequent extraction of these carriers. However, despite significant progress, the performance of PV cells is still low, leading to a cost/watt higher than the cost of traditional energy. For this reason, the evolution to the "next generation" solar cells is based on the high photoconversion efficiency (PCE) per unit area, with the theoretical possibility to approach the thermodynamic limit of 93% [1]. One of the major limitations to the efficiency of solar cell devices, however, is the mismatch between the spectral sensitivity of the active material and the solar spectrum, which is responsible for the loss of a significant part of radiation. Indeed, the absorption of radiation in photovoltaic solar cells is spectrally controlled by the bandgap (E_g) of the semiconductor material. For crystalline silicon (c-Si) solar cells, this corresponds to 1127 nm ($E_g = 1.1$ eV). Radiation with energy lower than the bandgap is not absorbed because it is not able to generate electron-hole pairs and it is lost. Radiation with energy higher than the gap is also not efficient because most of the energy is lost in internal thermalization processes or it is absorbed in the superficial region and the generated charge couples can recombine at surface defect states. Therefore, a way towards high efficiency devices is to improve the

* Corresponding author. Museo Storico della Fisica e Centro Studi e Ricerche Enrico Fermi, Piazza del Viminale 1, 00184 Roma, Italy and Division of Materials Science, Department of Engineering Sciences and Mathematics, Luleå University of Technology, 971 87 Luleå, Sweden.
E-mail address: francesco.enrichi@unive.it (F. Enrichi).

http://dx.doi.org/10.1016/j.optmat.2016.07.048

match between the solar spectrum and cell's absorption properties either by adjusting the band gap of the semiconductors to the solar spectrum, like in multi-junction cells, or by modifying the spectrum of the light that reaches the cell. The latter approach uses luminescent materials to transfer as much of the solar photon energies to the region of maximum absorption and efficiency of the device [2–4], close to the bandgap of the semiconductor. Rare earth (RE) ions are good luminescent candidates for this task [5,6], due to their wide variety of electronic levels, and Yb^{3+} ions are particularly suited for c-Si solar cells, due to the $^2F_{5/2} \rightarrow {}^2F_{7/2}$ transition which gives a NIR emission around 1000 nm. Moreover, co-doping with other RE ions has been widely studied for the possibility to enhance the Yb^{3+} efficiency via energy transfer and quantum cutting [7–9] and nanostructured RE doped glass-ceramics are among the most promising host materials for optical and photovoltaic applications [10–14].

In previous studies we used the sol gel method to develop RE doped silica-hafnia waveguides. In silica-hafnia glass-ceramics the rare earth ions are embedded in hafnia nanocrystals which have a cut-off frequency of about 700 cm^{-1}. Therefore the presence of hafnia nanocrystal produces a strong reduction of the non-radiative transition process reflected by a lengthening of the measured emission lifetime. Moreover, the sol gel preparation of silica-hafnia waveguides is a reliable and flexible system that was already proven to be suitable for rare earth doping [15,16]. Previous studies on $70SiO_2$–$30HfO_2$ downconverting waveguides by Tb^{3+}-Yb^{3+} codoping have already demonstrated to allow transfer efficiencies up to 55% [17,18]. Unfortunately these systems are still limited by the small absorption cross section and specific wavelengths of the RE ions involved, which limit the final performance of the process, while a strong and broadband conversion would be desirable, allowing the high efficiency conversion of a much wider part of the solar spectrum, in particular in the UV region, where the PV efficiency of the solar cell is small. A possible approach towards broadband and efficient energy conversion is the use of the energy transfer from semiconductor or metal nanostructures or nanocrystals to the RE ions. Noteworthy, this is not related to the exploitation of plasmonic effects [19,20], but rather to an efficient absorption followed by Förster energy transfer, which was widely investigated for Er^{3+} doped waveguide optical amplifiers [21–26], but never applied to Tb^{3+}-Yb^{3+} codoped glass ceramic waveguides for PV enhancement, to our knowledge.

In this paper we propose and test a cheap and easy method to dope with silver atoms glassy systems containing rare-earths, with the aim of combining the quantum cutting optical properties of rare-earth doped materials with broadband absorption and emission properties of silver aggregates such as single ions, dimers, trimers or small (charged or neutral) multimers [27] (extended reviews on this kind of structures obtained in silicate glass by Ag ion-exchange can be found in Refs. [28–36], as well as with possible energy-transfer mechanisms between metallic particles and rare earths, often shown in case of particle size less than 1–2 nm [37–39]. We report the synthesis and characterization of Tb^{3+}-Yb^{3+} codoped glass and glass ceramic waveguides, subsequently doped with Ag, focusing on the structural and optical properties of the obtained materials and on their potential application for high efficiency PV solar cells.

2. Experimental

Two series of $70SiO_2$–$30HfO_2$ samples in form of glass (G) or glass–ceramics (GC), depending on the final annealing treatment at 900 °C or 1000 °C, respectively, were activated by different molar concentrations of terbium and ytterbium ions and prepared by a sol–gel route using the dip-coating technique, keeping constant the ratio [Yb]/[Tb] = 4, following the experimental procedure described in Ref. [18]. Silica–hafnia films were deposited on cleaned pure SiO_2 substrates and the final films, obtained after 20 dips, were stabilized by a treatment of 5 min in air at 900 °C. As a result of the procedure, transparent and crack-free films were obtained (TY-G sample). To obtain GC samples, an additional heat treatment was performed in air at a temperature of 1000 °C for 30 min in order to nucleate hafnia nanocrystals inside the film (TY-GC sample). $70SiO_2$–$30HfO_2$ GC planar waveguides doped with rare earth ions were thus produced. A glass sample with only Tb was also prepared (T0-G).

To introduce Ag in the Tb/Yb codoped waveguides, a doping was performed by immersing the samples in a molten salt bath (1 mol% of $AgNO_3$ in $NaNO_3$) as for the ion exchange in glasses [27,34,40]. The bath temperature was 350 °C, for 1 h of immersion duration. In order to favour the possible formation of small Ag aggregates, different annealing in air were performed after the silver doping: 1 h at 380 °C or 1 h at 440 °C. The sample labels, their thickness and refractive index at 544 nm and 632 nm are reported in Table 1.

Thickness and refractive index (at 544 and 632 nm) of the waveguides were obtained by a variable angle Woollam V-VASE spectroscopic ellipsometer. Elemental profiling was done by Secondary Ion Mass Spectrometry (SIMS) in ultra-high vacuum conditions at different primary beam intensities (50 nA and 75 nA), rastering over a nominally 125 × 125 μm^2 area. The beam-blanking mode was used to improve the depth resolution, interrupting the sputtering process during magnet stabilization periods. The dependence of the erosion speed on the matrix composition was experimentally tested by measuring the depth of the erosion crater at the end of each analysis by means of a Tencor Alpha Step profiler with a maximum uncertainty of a few nanometers. The measurements were performed in high mass resolution configuration to avoid mass-interference artefacts. The charge build-up while profiling the insulating samples was compensated by an electron gun without any need to cover the surface with a metal film.

Elemental concentration was obtained by Rutherford Backscattering Spectrometry (RBS) at INFN-Legnaro National Laboratories by using a 2.0 MeV $^4He^+$ beam (backscattering angle = 160°). The atoms concentration was calculated by simulating the RBS spectra with the RUMP code.

Photoluminescence (PL) characterization was done by a Horiba JobinYvon Fluorolog-3 spectrofluorimeter in the whole range UV–VIS–NIR wavelengths. The light of a 450 W Xenon lamp excites the sample after passing a double-grating Czerny–Turner monochromator to select the desired wavelength. The optical emission of the sample is analysed by a single grating monochromator coupled to a suitable detector: a Hamamatsu PMT R928 for measurements between 185 nm and 900 nm or a PMTR5509-73 for measurements up to 1700 nm.

3. Result and discussion

3.1. Structural investigation

The structural investigation of the glass and glass-ceramic samples was already reported in Ref. [18], demonstrating the formation of few nanometre sized HfO_2 nanocrystals in an amorphous silica matrix only after 1000 °C annealing treatments (TY-GC series), while the matrix remains amorphous for 900 °C annealing (T0-G and TY-G series). As an example of Ag-doped samples, in Fig. 1 the RBS analysis of the T0-G-A as-doped sample is shown, with the corresponding simulation curve. The curve is in good agreement with the nominal composition of the material and attests the presence of a small, but measurable, amount of Ag of the order of (0.2 ± 0.1) at.%. After annealing, the presence of Ag was

Table 1
Samples label, synthesis conditions, thickness, and refractive index measured at 544 nm and 632 nm. Thickness and refractive index uncertainties are 5 nm and 0.002, respectively.

Label sample	[Tb] mol%	[Yb] mol%	Ag doping	Annealing T (°C)	Thickness (nm)	n@544	n@632
T0-G	1	0	–	–	705	1.626	1.621
T0-G-A	1	0	✓	–	665	1.670	1.662
T0-G-B	1	0	✓	380	665	1.684	1.675
T0-G-C	1	0	✓	440	670	1.666	1.658
TY-G	1	4	–	–	710	1.641	1.634
TY-G-A	1	4	✓	–	695	1.678	1.673
TY-G-B	1	4	✓	380	675	1.709	1.703
TY-G-C	1	4	✓	440	690	1.700	1.697
TY-GC	1	4	–	–	655	1.677	1.672
TY-GC-A	1	4	✓	–	660	1.676	1.671
TY-GC-B	1	4	✓	380	650	1.693	1.689
TY-GC-C	1	4	✓	440	655	1.683	1.678

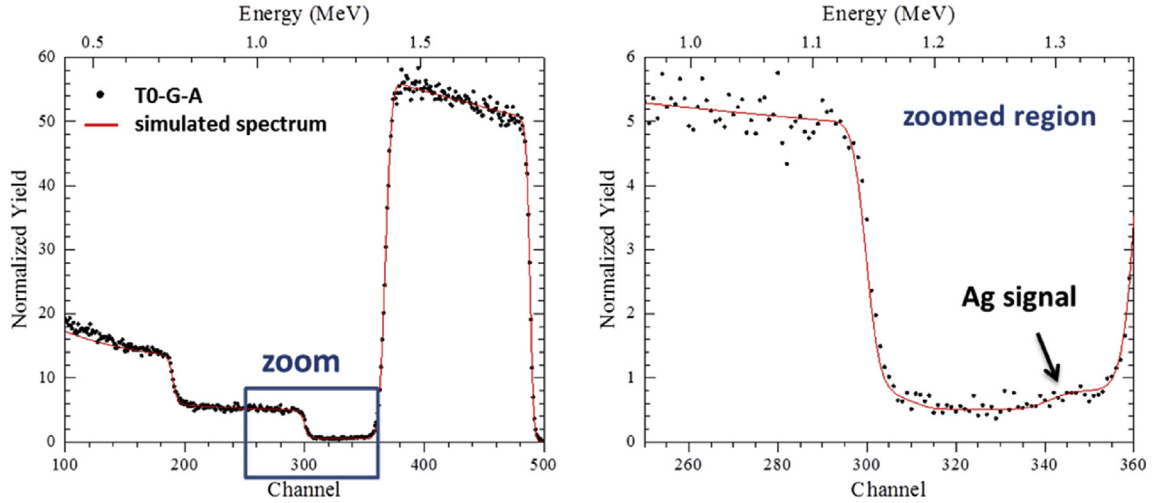

Fig. 1. RBS spectrum of T0-G-A sample and corresponding simulation curve. On the right, the zoomed region points out the presence of a small 0.2 at.% amount of Ag.

strongly reduced. For all the glass-ceramic samples Ag was not detectable at all.

The observed behaviour was confirmed by SIMS analysis. As an example, the elemental profiles acquired for the T0-G-A sample are reported in Fig. 2. For each element, the signal is proportional to the concentration and the integral of the curve is proportional to the total amount of the specific element. In the figure, the waveguide/substrate interface is also indicated as a vertical dashed line. The thicknesses of the waveguides evaluated by SIMS are in agreement with the ellipsometric measurements reported in Table 1.

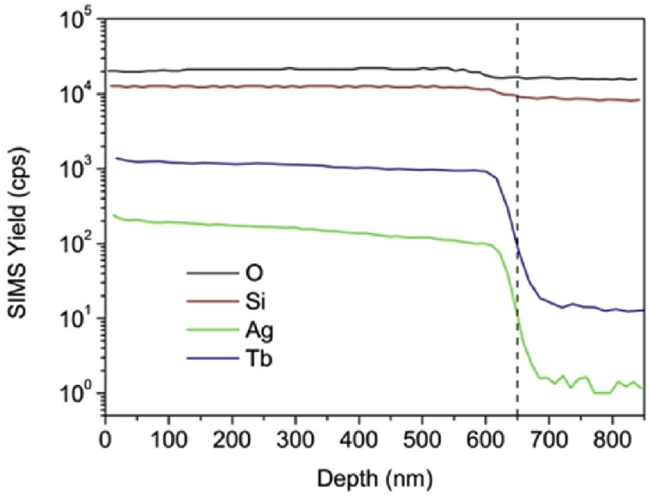

Fig. 2. SIMS elemental profiles for the T0-G-A sample, with indication of the waveguide/substrate interface (vertical dashed line).

The SIMS measurements on the glass samples confirm the introduction of Ag in the whole waveguide. The mobility of Ag in the glass is evidenced by SIMS before and after the annealing treatments. Indeed, after annealing at 380 °C and 440 °C, the Ag depth profile does not change its shape but the total amount of silver decreases at the 40% of the starting value, suggesting an out-diffusion process. A completely different behaviour was found for glass-ceramic samples (GC), where the Ag signal was not detected. The mentioned SIMS results are in very good agreement with RBS measurements. The lacking of silver in GC samples could be expected considering that the GC samples have a more compact structure than the glassy ones, therefore reducing or preventing the in-depth Ag diffusion.

3.2. Optical and photoluminescence analysis

The optical characterization results for the prepared samples in terms of refractive index and thickness of the waveguides obtained

by ellipsometry are reported in Table 1. The waveguides have a thickness between 0.6 and 0.7 μm and their refractive index confirms what observed by the previous structural analysis. Indeed the Ag doping process is more effective for the G samples, attested by a significant stronger increase of the index of refraction, while it has a relatively small effect on the GC samples, where the index of refraction is almost unchanged.

Fig. 3 reports the PL emission in the visible region of TY-G and TY-GC series of samples before and after Ag introduction and subsequent thermal treatment (by exciting the samples at 377 nm). The intense emission from $^5D_4 \rightarrow {}^7F_5$ Tb^{3+} transition at 543.5 nm can be clearly detected. Moreover, only for the G samples, a very intense broadband emission in the violet-blue spectral region appears as the dominant feature after the Ag doping process, but it is strongly reduced after the subsequent thermal treatment. In particular, the band presents two emission peaks centred at 415 nm and 436 nm (3.0 and 2.8 eV, respectively). In agreement with SIMS, RBS and ellipsometry measurements, we can reasonably attribute the appearing of this emission to the effective introduction of Ag in the matrix. Further luminescence investigation is reported in Fig. 4 by exciting the samples at 280 nm wavelength. It is worth observing that the spectral emission of the violet-blue band is almost unchanged, i.e. shape and position remained the same. The analysis on the GC sample series reports only the spectral emission features related to $^5D_4 \rightarrow {}^7F_J$ ($J = 2–6$) transitions of Tb^{3+} ions: this is related to the already evidenced ineffective introduction of silver in the glass-ceramic matrices.

The PLE spectra for G and GC samples are reported in Fig. 5 and Fig. 6, respectively, for two different emission wavelengths (450 nm and 543.5 nm). When the emission at 543.5 nm is observed, the typical direct excitation peaks of Tb^{3+} ions are detected. Only for the TY-G-A sample, a broad excitation band is also present, around 400 nm. This band is much higher and better evidenced by observing the emission at 450 nm, showing an excitation maximum at 366 nm (3.4 eV) and a shoulder around 280 nm (4.4 eV) (Fig. 5).

In principle, photoluminescence excitation and emission spectra from Ag species can provide information concerning the metal aggregation process, as mentioned before; at the same time, the analysis of Tb^{3+} and Yb^{3+} emissions can be used to detect the occurrence of possible sensitization, enhancement and energy transfer from Ag aggregates to the rare earth ions. The intense emission in the 400–450 nm range, showed by the TY-G-A sample (Fig. 3), could be associated to interactions between ions constituting Ag^+–Ag^+ pairs [27,31–34,41–44]. However, by changing the excitation wavelength we observed an unexpected stability of

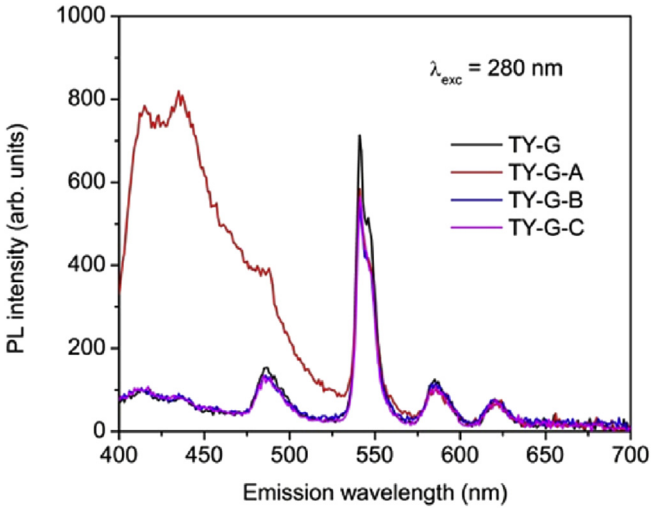

Fig. 4. Photoluminescence emission spectra for the TY-G (left) and TY-GC (right) samples before and after Ag-exchange and annealing; excitation wavelength is 280 nm.

shape and position of these bands (Fig. 4), as already mentioned, suggesting that they could not be completely related to the reported silver structures, whose emissions usually red-shift by decreasing the excitation wavelength [see for instance: 27,31]. Actually, a very similar emission in the 400–450 nm range was evidenced in synthetic silica [45], and in particular in sol-gel derived pure silica [46,47], being related to oxygen-deficiency centers (ODCs). Moreover, in Ag-doped silica the same emission was detected much more intense than in pure silica [48], suggesting that the Ag doping of our silica-based waveguides - producing mainly Ag ions which compete with the other cations for the available oxygen atoms - probably creates a large number of ODCs in the glass network as a consequence of the depolymerization of the structure. In this frame, the ODCs formation related to the silver atoms entering the matrix suggests that the doping process is the consequence of a thermal diffusion rather than of an ion exchange.

Due to the very low Ag concentration, we can expect that Ag is mainly isolated and the presence of multimers could be reasonably excluded. After annealing, a significant out-diffusion of Ag from the sample, attested by SIMS, and a general rearrangement of the matrix as a consequence of the annealing in oxygen-rich atmosphere (air) can explain the disappearance of the PL emission band mainly related to ODCs.

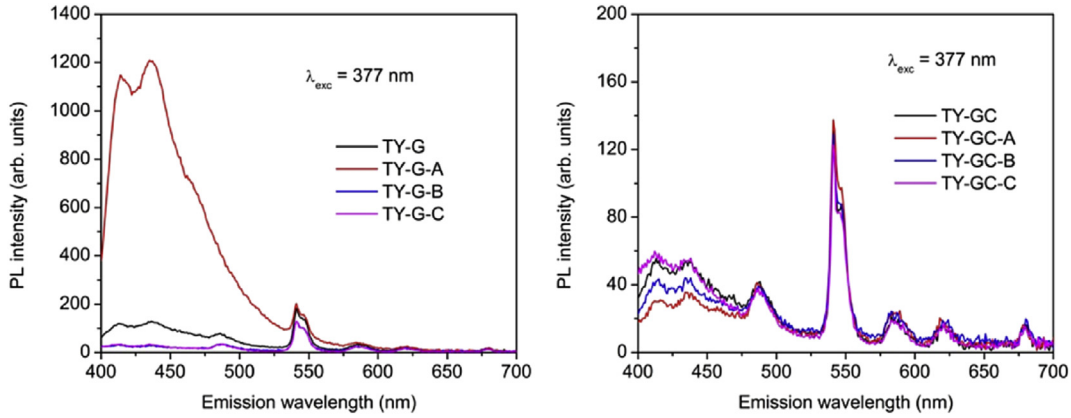

Fig. 3. Photoluminescence emission spectra for the TY-G (left) and TY-GC (right) samples before and after Ag-exchange and annealing; excitation wavelength is 377 nm.

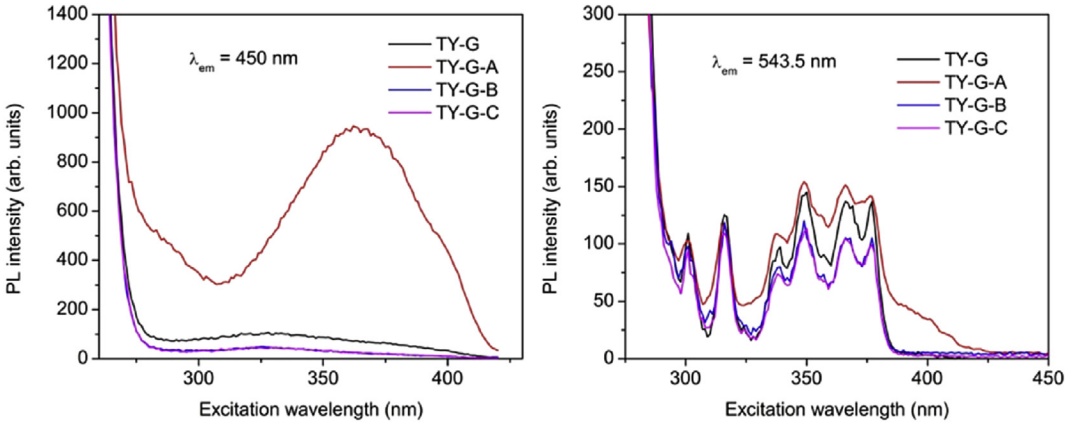

Fig. 5. Photoluminescence excitation spectra for the TY-G samples at 450 nm (left) and 543.5 nm (right) before and after Ag-exchange and annealing.

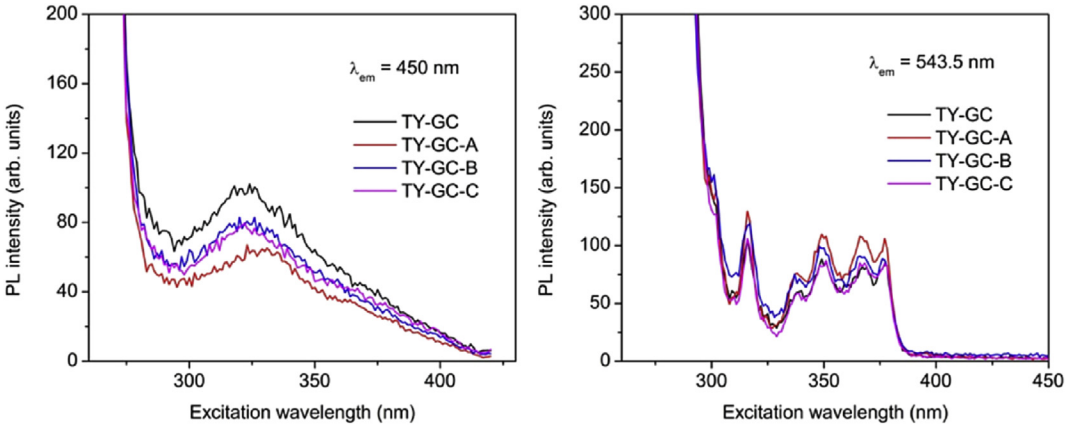

Fig. 6. Photoluminescence excitation spectra for the TY-GC samples at 450 nm (left) and 543.5 nm (right) before and after Ag-exchange and annealing.

The emission in the 400–450 nm range is widely extended in the whole near-UV region and could provide a significant contribution for enhancing the efficiency of solar cells, downshifting the solar spectrum from near-UV to the visible; the combination with Tb^{3+} and Yb^{3+} rare earth ions can further shift the emitted wavelength to the region of best absorption of the cell. It was not possible, however, to clearly prove the energy transfer (ET) between Ag-induced ODCs and rare-earth ions, probably due to the very low amount of silver introduced: the ET, on the contrary, was evident in Tb:SiO_2 systems for Ag doping as high as 1 mol % [48].

4. Conclusions

This paper reports on the possibility to introduce Ag in 1% Tb^{3+}–4%Yb^{3+} doped glass (G) and glass-ceramic (GC) sol-gel silica-hafnia waveguides by immersion in molten salt bath. The films were prepared by sol-gel deposition, annealing at 900 °C (G) or 1000 °C (GC), and subsequent immersion in a molten salt bath containing 1 mol% of silver followed by a final thermal treatment in air at 380 °C or 440 °C. RBS and SIMS analyses showed the successful introduction of Ag for the G films, but the silver total amount was limited to approximately 0.2 at.%. Moreover, the following thermal treatments further reduce the Ag amount at 40% of the starting value. On the contrary, Ag was not detected in the GC films. PL analysis of the as-exchanged G sample evidenced a strong broadband UV excitation centred at 365 nm and extending up to 420 nm, responsible for an intense blue emission, which can be reasonably ascribed to oxygen-deficiency centers induced by the silver presence and – to a less extent – to Ag^{+}–Ag^{+} interactions. This emission completely disappears after annealing, due to the reduction of the Ag amount and/or changing of Ag aggregation form, and was not detected at all in GC samples. Controlling the spectral features of this band and combining it with absorption and emission of other rare earths like Tb and Yb could be very interesting for increasing solar cells efficiency by downshifting UV radiation into the visible and more. Further work will be focused on increasing the Ag concentration in the films to better clarify the role of this element and its interaction with the silica-hafnia matrix and, as a consequence, with the embedded rare earth ions.

Acknowledgments

The research activity was performed in the framework of the CNR-CNRST joint project (2014–2015), CNR-PAS joint project (2014–2016), and the PLESC project “Plasmonics for a better efficiency of solar cells” between South Africa and Italy (contributo del Ministero degli Affari Esteri e della Cooperazione Internazionale, Direzione Generale per la Promozione del Sistema Paese). F.E. acknowledges VINNOVA, under the Vinnmer Marie Curie Incoming - Mobility for Growth Programme (project “Nano2solar” Ref. N. 2016-02011).

References

[1] M.A. Green, Third Generation Photovoltaics: Advanced Solar Energy Conversion, Springer-Verlag, Berlin Heidelberg, 2003.
[2] C. Strumpel, M. McCann, G. Beaucarne, V. Arkhipov, A. Slaoui, V. Švrček, C. del

Cañizo, I. Tobias, Modifying the solar spectrum to enhance silicon solar cell efficiency - an overview of available materials, Sol. Energy Mater. Sol. Cells 91 (2007) 238–249.
[3] B.S. Richards, Luminescent layers for enhanced silicon solar cell performance: down-conversion, Sol. Energy Mater. Sol. Cells 90 (2006) 1189–1207.
[4] A. Shalav, B.S. Richards, M.A. Green, Luminescent layers for enhanced silicon solar cell performance: up-conversion, Sol. Energy Mater. Sol. Cells 91 (2007) 829–842.
[5] A. Meijerink, R. Wegh, P. Vergeer, T. Vlught, Photon management with lanthanides, Opt. Mater 28 (2006) 575–581.
[6] G. Liu, B. Jacquier, Spectroscopic Properties of Rare Earths in Optical Materials, Springer-Verlag, Berlin Heidelberg, 2005.
[7] L. Guo, Y. Wang, W. Zeng, L. Zhao, L. Han, "Band structure and near infrared quantum cutting investigation of GdF3:Yb3+, Ln3+ (Ln = Ho, Tm, Er, Pr, Tb) nanoparticles, Phys. Chem. Chem. Phys. 15 (2013) 14295–14302.
[8] L. Aarts, B.M. van der Ende, A. Meijerink, Downconversion for solar cells in NaYF4 :Er,Yb, J. Appl. Phys. 106 (2009) 023522, 1–6.
[9] W.J. Park, S.J. Oh, J.K. Kim, J. Heo, T. Wagner, L. Strizik, Down-conversion in Tm3+/Yb3+ doped glasses for multicrystalline silicon photo-voltaic module efficiency enhancement, J. Non Cryst. Solids 383 (2014) 181–183.
[10] D.H. Li, Y.J. Chen, J.H. Huang, X.H. Gong, Y.F. Lin, Z.D. Luo, Y.D. Huang, Near-infrared down-conversion in Pr3+–Yb3+ co-doped transparent glass ceramic containing Ca5(PO4)3F nanocrystals, Phys. B 446 (2014) 12–16.
[11] M.C. Gonçalves, L.F. Santos, R.M. Almeida, Rare-earth-doped transparent glass ceramics, Comptes Rendus Chim. 5 (2002) 845–854.
[12] S. Ye, Y. Katayama, S. Tanabe, Down conversion luminescence of Tb3+–Yb3+ codoped SrF2 precipitated glass ceramics, J. Non Cryst. Solids 357 (2011) 2268–2271.
[13] S. Ye, B. Zhu, J. Chen, J. Luo, J.R. Qiu, Infrared quantum cutting in Tb3+,Yb3+ codoped transparent glass ceramics containing CaF2 nanocrystals, Appl. Phys. Lett. 92 (2008) 141112, 1–3.
[14] S. Berneschi, S. Soria, G.C. Righini, G. Alombert-Goget, A. Chiappini, A. Chiasera, Y. Jestin, M. Ferrari, S. Guddala, E. Moser, S.N.B. Bhaktha, B. Boulard, C. Duverger Arfuso, S. Turrell, Rare-earth-activated glass–ceramic waveguides, Opt. Mater 32 (2010) 1644–1647.
[15] Y. Jestin, C. Armellini, A. Chiappini, A. Chiasera, M. Ferrari, C. Goyes, M. Montagna, E. Moser, G. Nunzi Conti, S. Pelli, R. Retoux, G.C. Righini, G. Speranza, Erbium activated HfO2 based glass–ceramics for photonics, J. Non Cryst. Solids 353 (2007) 494–497.
[16] Y. Jestin, C. Armellini, A. Chiasera, A. Chiappini, M. Ferrari, E. Moser, R. Retoux, G.C. Righini, Low-loss optical Er3+-activated glass-ceramics planar waveguides fabricated by bottom-up approach, Appl. Phys. Lett. 91 (2007) 071909, 1–3.
[17] G. Alombert-Goget, C. Armellini, S. Berneschi, A. Chiappini, A. Chiasera, M. Ferrari, S. Guddala, E. Moser, S. Pelli, D.N. Rao, G.C. Righini, Tb3+/Yb3+ co-activated Silica-Hafnia glass ceramic waveguides, Opt. Mater 33 (2010) 227–230.
[18] A. Bouajaj, S. Belmokhtar, M.R. Britel, C. Armellini, B. Boulard, F. Belluomo, A. Di Stefano, S. Polizzi, A. Lukowiak, M. Ferrari, F. Enrichi, Tb3+/Yb3+ codoped silica–hafnia glass and glass–ceramic waveguides to improve the efficiency of photovoltaic solar cells, Opt. Mater 52 (2016) 62–68.
[19] H.A. Atwater, A. Polman, Plasmonics for improved photovoltaic devices, Nat. Mater 9 (2010) 205–213.
[20] M.A. Green, S. Pillai, Harnessing plasmonics for solar cells, Nat. Photonics 6 (2012) 130–132.
[21] A. Martucci, M. De Nuntis, A. Ribaudo, M. Guglielmi, S. Padovani, F. Enrichi, G. Mattei, P. Mazzoldi, C. Sada, E. Trave, G. Battaglin, G. Gonella, E. Borsella, M. Falconieri, M. Patrini, J. Fick, Silver-sensitized erbium-doped ion-exchanged sol–gel waveguides, Appl. Phys. A 80 (2005) 557–563.
[22] F. Enrichi, G. Mattei, C. Sada, E. Trave, D. Pacifici, G. Franzò, F. Priolo, F. Iacona, M. Prassas, M. Falconieri, E. Borsella, Evidence of energy transfer in an aluminosilicate glass codoped with Si nanoaggregates and Er3+ ions, J. Appl. Phys. 96 (2004) 3925–3932.
[23] A. Chiasera, M. Ferrari, M. Mattarelli, M. Montagna, S. Pelli, H. Portales, J. Zheng, G.C. Righini, Assessment of spectroscopic properties of erbium ions in a soda-lime silicate glass after silver–sodium exchange, Opt. Mater 27 (2005) 1743–1747.
[24] F. Gourbilleau, C. Dufour, M. Levalois, J. Vicens, R. Rizk, C. Sada, F. Enrichi, G. Battaglin, Room-temperature 1.54 μm photoluminescence from Er-doped Si-rich silica layers obtained by reactive magnetron sputtering, J. Appl. Phys. 94 (2003) 3869–3874.
[25] C. Strohhofer, A. Polman, Silver as a sensitizer for erbium, Appl. Phys. Lett. 81 (2002) 1414–1416.
[26] M. Mattarelli, M. Montagna, K. Vishnubhatla, A. Chiasera, M. Ferrari, G.C. Righini, Mechanisms of Ag to Er energy transfer in silicate glasses: a photoluminescence study, Phys. Rev. B 75 (2007) 125102, 1–6.
[27] E. Cattaruzza, V.M. Caselli, M. Mardegan, F. Gonella, G. Bottaro, A. Quaranta, G. Valotto, F. Enrichi, Ag+↔Na+ ion exchanged silicate glasses for solar cells covering: down-shifting properties, Ceram. Intern 41 (2015) 7221–7226.
[28] T.G. Giallorenzi, E.J. West, R. Kirk, R. Ginther, R.A. Andrews, Optical waveguides formed by thermal migration of ions in glass, Appl. Opt. 12 (1973) 1240–1245.
[29] R.V. Ramaswamy, R. Srivastava, Ion exchanged glass waveguides: a review, J. Light. Technol. 6 (1988) 984–1002.
[30] S.I. Najafi, Introduction to Glass Integrated Optics, Artech House, Boston-London, 1992.
[31] E. Cattaruzza, M. Mardegan, E. Trave, G. Battaglin, P. Calvelli, F. Enrichi, F. Gonella, Modifications in silver-doped silicate glasses induced by ns laser beams, Appl. Surf. Sci. 257 (2011) 5434–5438.
[32] E. Borsella, G. Battaglin, M.A. Garcia, F. Gonella, P. Mazzoldi, R. Polloni, A. Quaranta, Structural incorporation of silver in soda-lime glass by the ion-exchange process: a photoluminescence spectroscopy study, Appl. Phys. A 71 (2000) 125–132.
[33] E. Borsella, F. Gonella, P. Mazzoldi, A. Quaranta, G. Battaglin, R. Polloni, Spectroscopic investigation of silver in soda-lime glass, Chem. Phys. Lett. 284 (1998) 429–434.
[34] A. Simo, J. Polte, N. Pfänder, U. Vainio, F. Emmerling, K. Rademann, Formation mechanism of silver nanoparticles stabilized in glassy matrices, J. Am. Chem. Soc. 134 (2012) 18824–18833.
[35] J. Li, Y. Yang, D. Zhou, Z. Yang, X. Xu, J. Qiu, Investigation of the role of silver species on spectroscopic features of Sm3+-activated sodium–aluminosilicate glasses via Ag+-Na+ ion exchange, J. Appl. Phys. 113 (2013) 193103.
[36] S. Lai, Z. Yang, J. Li, B. Shao, J. Yang, Y. Wang, J. Qiu, Z. Song, J. Mater. Chem. C 3 (2015) 7699–7708.
[37] E. Cattaruzza, G. Battaglin, F. Visentin, E. Trave, G. Aquilanti, G. Mariotto, Enhanced photoluminescence at λ=1.54 μm in Cu-doped Er:SiO2 system, J. Phys. Chem. C 116 (2012) 21001–21011.
[38] C. Maurizio, E. Trave, G. Perotto, V. Bello, D. Pasqualini, P. Mazzoldi, G. Battaglin, T. Cesca, C. Scian, G. Mattei, Phys. Rev. B 83 (2011) 195430.
[39] D. Pacifici, G. Franzò, F. Priolo, F. Iacona, L. Dal Negro, Phys. Rev. B 67 (2003) 245301.
[40] A. Quaranta, E. Cattaruzza, F. Gonella, Modelling the ion exchange process in glass: phenomenological approaches and perspectives, Mat. Sci. Eng. B 149 (2008) 133–139.
[41] A. Quaranta, A. Rahman, G. Mariotto, C. Maurizio, E. Trave, F. Gonella, E. Cattaruzza, E. Ghibaudo, J.E. Broquin, Spectroscopic investigation of structural rearrangements in silver ion-exchanged silicate glasses, J. Phys. Chem. C 116 (2012) 3757–3764.
[42] J.A. Jimenez, S. Lysenko, G. Zhang, H. Liu, Optical properties of silver-doped aluminophosphate glasses, J. Mater. Sci. 42 (2007) 1856–1863.
[43] E. Borsella, E. Cattaruzza, G. De Marchi, F. Gonella, G. Mattei, P. Mazzoldi, A. Quaranta, G. Battaglin, R. Polloni, J. Non Cryst. Solids 245 (1999) 122–128.
[44] E. Cattaruzza, M. Mardegan, T. Pregnolato, G. Ungaretti, G. Aquilanti, A. Quaranta, G. Battaglin, E. Trave, Ion exchange doping of solar cell coverglass for sunlight down-shifting, Sol. Energy Mater. Sol. Cells 130 (2014) 272–280.
[45] L. Skuja, Optically active oxygen-deficiency-related centers in amorphous silicon dioxide, J. Non Cryst. Solids 239 (1998) 16–48.
[46] J. Lin, K. Baerner, Tunable photoluminescence in sol–gel derived silica xerogels, Mater. Lett. 46 (2000) 86–92.
[47] A.E. Abbass, H.C. Swart, R.E. Kroon, White luminescence from sol–gel silica doped with silver, J. Sol-Gel Sci. Technol. 76 (2015) 708–714.
[48] A.E. Abbass, H.C. Swart, R.E. Kroon, Effect of silver ions on the energy transfer from host defects to Tb ions in sol–gel silica glass, J. Luminescence 160 (2015) 22–26.